Chapter 7

Finite-Time Discrete Control for Two-DOF Helicopter System

7.1 Introduction

In the past few decades, unmanned aerial vehicles and helicopters have seen a surge in popularity due to their demand in various sectors, such as trans-shipment, defense, emergency response, police operations, and drone imagery [59]. The discrete control methodologies, extensively explored in a range of articles [60–62]. The discrete-time approach emerges as notably superior to continuous-time emulation in terms of both stability and achievable performances. Most of the available techniques for feedback stabilization of discrete-time systems (DTS) lead to closed-loop systems that guarantee exponential convergence with an infinite settling time [10, 63]. While these methods demonstrate efficacy, exploring finite-time discrete algorithms holds promise for enhanced performance. Recently, in [64] and [20], authors have established finite-time stabilization for discrete autonomous systems based on a minimum operator, and later its application was developed in discrete sliding mode control [65, 66]. Expanding on the concepts outlined in [20], the researchers in [11] investigate finite-time control strategies for high-order discrete-time nonlinear systems. They develop a method for designing finite-time controllers using a recursive computation approach grounded in backstepping principles.

Certainly, the realm of control design grounded in discrete finite-time stability has entered a new frontier, particularly in the domain of rated convergence for discrete-time systems (DTS). However, there are no results pertaining to discrete finite-time stabiliza-

tion of two-DOF helicopters. Based on the above observations, we study the backstepping-based discrete finite-time control of a two-DOF helicopter for desired reference tracking.

It is crucial to note that employing backstepping procedures for finite-time stabilization of two-DOF helicopters introduces future state information of the virtual control signal, raising concerns about causality violation and the potential failure to achieve the designed control scheme. To address the causality problem inherent in backstepping procedures for finite-time stabilization, a new finite-time backstepping control technique is proposed in [11] where the finite-time stability analysis is given from the last subsystem to the first subsystem, and the settling time can be estimated.

Expanding upon the principles explored in [11, 20], this chapter presents a discrete finite-time control approach aimed at accomplishing finite-time trajectory tracking for a two-degree-of-freedom (2-DOF) helicopter system. The primary contributions of this research are summarized as follows:

1. Departing from conventional continuous-time and asymptotically convergent control methods applied to nonlinear two-DOF helicopter systems [10, 63, 67, 68], this study marks the first substantial effort in investigating discrete finite-time control of two-DOF helicopter system. The approach leverages the finite-time Lyapunov stability theorem, introducing a paradigm shift in addressing the challenges associated with these complex systems.

2. In alignment with the methodology proposed in [11] and [10], the causality contradiction is effectively managed through a recursive backstepping approach, enabling the acquisition of future information.

3. In contrast to conventional control methods, this study introduces a technique for estimating the settling time of the two-degree-of-freedom (2-DOF) helicopter system by examining finite-time stability, starting from the last subsystem and progressing to the first.

7.2 Two-DOF Helicopter System Description

In this study, we focus on the two-DOF helicopter system. Utilizing the Euler-Lagrangian equation, the subsequent continuous-time mathematical representation is expressed as

Figure 7.1: Experimental setup of two-DOF helicopter.

follows:

$$\ddot{\theta}_1(t) = -\frac{B_p\dot{\theta}_1(t)}{J_{pp} + m_{heli}l^2} + \frac{m_{heli}l^2\dot{\theta}_2^{\,2}(t)\sin(\theta_1)\cos(\theta_1)}{J_{pp} + m_{heli}l^2} - \frac{m_{heli}gl\cos(\theta_1)}{J_{pp} + m_{heli}l^2} + \frac{K_{pp}V_p}{J_p + m_{heli}l^2} + \frac{K_{py}V_y}{J_{pp} + m_{heli}l^2} \tag{7.1}$$

$$\ddot{\theta}_2(t) = \frac{2m_{heli}l^2\dot{\theta}_2(t)\sin(\theta_1)\cos(\theta_1)\dot{\theta}_1(t)}{J_{yy}} - \frac{B_y\dot{\theta}_2(t)}{J_{yy}} + \frac{K_{yp}V_p}{J_{yy}} + \frac{K_{yy}V_y}{J_{yy}} \tag{7.2}$$

Here, $\theta_1(t)$, $\dot{\theta}_1(t)$, $\theta_2(t)$, and $\dot{\theta}_2(t)$ correspond to the pitch angle, pitch velocity, yaw angle, and yaw velocity, respectively. The input voltages applied to the pitch and yaw motors are represented as V_p and V_y. Additional details regarding the system parameters can be accessed in [68].

The mathematical model presented above for the two-DOF helicopter system is described in continuous time [68]. However, in the current study, we adopt a discrete-time approach. Consequently, we propose the discretization of the helicopter model using

the Euler discretization technique [69].

$$x_1(k+1) = x_1(k) + x_2(k)h \tag{7.3}$$

$$\begin{aligned} x_2(k+1) = {} & x_2(k) - c_1\cos(x_1(k))h - c_2x_2(k)h \\ & + c_4hV_p(k) - c_3\sin(x_1(k))\cos(x_1(k))x_4^2(k)h \\ & + c_5hV_y(k) \end{aligned} \tag{7.4}$$

$$x_3(k+1) = x_3(k) + x_4(k)h \tag{7.5}$$

$$\begin{aligned} x_4(k+1) = {} & x_4(k) - c_6x_4(k)h + c_8hV_p(k) + c_9hV_y(k) \\ & + c_7\sin(x_1(k))\cos(x_1(k))x_2(k)x_4(k)h. \end{aligned} \tag{7.6}$$

where h is the sampling period and the constant parameters c_i, $i = 1, \ldots, 9$ are expressed as,

$$\begin{aligned} c_1 &= \frac{m_{heli}gl_{cm}}{J_{pp} + m_{heli}l_{cm}^2}, \quad c_2 = \frac{B_p}{J_{pp} + m_{heli}l_{cm}^2}, \\ c_3 &= \frac{m_{heli}l_{cm}^2}{J_{pp} + m_{heli}l_{cm}^2}, \quad c_4 = \frac{K_{pp}}{J_{pp} + m_{heli}l_{cm}^2}, \\ c_5 &= \frac{K_{py}}{J_{pp} + m_{heli}l_{cm}^2}, \quad c_6 = \frac{B_y}{J_{yy}} \\ c_7 &= \frac{2m_{heli}l_{cm}^2}{J_{yy}}, \quad c_8 = \frac{K_{yp}}{J_{yy}}, \quad c_9 = \frac{K_{yy}}{J_{yy}}. \end{aligned}$$

In this configuration, $x_1(k)$ denotes the angle on the pitch axis, while $x_3(k)$ signifies the angle on the yaw axis. A positive pitch position corresponds to the helicopter's nose elevating, and a positive yaw position indicates a clockwise rotation. The velocities in the pitch and yaw axes are represented by $x_2(k)$ and $x_4(k)$, respectively. The voltage input for the pitch motor is given by $V_p(k)$, and for the yaw motor, it is $V_y(k)$. In order to simplify further analysis, we set $h = 1$.

The goal is to formulate the control laws for $u_p(k)$ and $u_y(k)$ such that the outputs $x_1(k)$ and $x_3(k)$ align with the desired reference signals $x_{1d}(k)$ and $x_{3d}(k)$, respectively, within a finite time. Rewriting equations (7.3)-(7.6) into the state space form, we get

$$x_1(k+1) = x_1(k) + x_2(k) \tag{7.7}$$

$$x_2(k+1) = x_2(k) + \phi_1(x(k))^T\eta_1 + u_p(k) \tag{7.8}$$

$$x_3(k+1) = x_3(k) + x_4(k) \tag{7.9}$$

$$x_4(k+1) = x_4(k) + \phi_2(x(k))^T\eta_2 + u_y(k) \tag{7.10}$$

where

$$\phi_1(x(k)) = \begin{bmatrix} -\cos(x_1(k)) \\ -x_2(k) \\ -\cos(x_1(k))\sin(x_1(k))x_4^2(k) \end{bmatrix}, \eta_1 = \begin{bmatrix} c_1 \\ c_2 \\ c_3 \end{bmatrix},$$

$$\phi_2(x(k)) = \begin{bmatrix} -x_4(k) \\ x_2(k)x_4(k)\cos(x_1(k))\sin(x_1(k)) \end{bmatrix}, \eta_2 = \begin{bmatrix} c_6 \\ c_7 \end{bmatrix}.$$

and $u_p(k)$ and $u_y(k)$ as the control inputs for the pitch and yaw motor, respectively, defined as:

$$u_p(k) = c_4 V_p(k) + c_5 V_y(k) \tag{7.11}$$

$$u_y(k) = c_8 V_p(k) + c_9 V_y(k) \tag{7.12}$$

The future information of the reference signal $x_{di}(k)$ is assumed to be known, bounded, and piecewise continuous.

Remark 7.1 *Please note that the future reference signal $x_{di}(k+d)$ is required to implement the controller. In practice, the trajectory to be tracked is usually predefined in tracking applications. Thus, $x_{di}(k+d)$ is known a priori.*

7.3 Finite-Time Discrete Control Design

We will employ the recursive backstepping technique to design a finite-time feedback control law for the two-DOF helicopter system (7.7)-(7.10). To initiate this process, we will first apply a change of coordinates to transform the state variables as follows:

$$z_1(k) = x_1(k) - x_{1d}(k) \tag{7.13}$$

$$z_2(k) = x_2(k) - \alpha_1(k) \tag{7.14}$$

$$z_3(k) = x_3(k) - x_{3d}(k) \tag{7.15}$$

$$z_4(k) = x_4(k) - \alpha_2(k) \tag{7.16}$$

where $\alpha_1(k)$ and $\alpha_2(k)$ are virtual control signals. Choose $\alpha_1(k)$ and $\alpha_2(k)$ as

$$\alpha_1(k) = f_1(z_1(k)) = -x_{1d}(k) + x_{1d}(k+1) - c\min\left(\frac{|z_1(k)|}{c}, |z_1(k)|^\gamma\right) \tag{7.17}$$

$$\alpha_2(k) = f_2(z_3(k)) = -x_{3d}(k) + x_{3d}(k+1) - c\min\left(\frac{|z_3(k)|}{c}, |z_3(k)|^\gamma\right) \tag{7.18}$$

where $c > 0$ and $\gamma \in (0, 1)$ be positive design constants. With these, the transformed dynamics can be expressed as:

$$z_1(k+1) = z_1(k) + z_2(k) + x_{1d}(k) - x_{1d}(k+1) + \alpha_1(k) \tag{7.19}$$

$$z_2(k+1) = z_2(k) + f_1(z_1(k)) - f_3(z_1(k), z_2(k)) + u_p(k) + \phi_1(x(k))\eta_1 \tag{7.20}$$

$$z_3(k+1) = z_3(k) + z_4(k) + x_{3d}(k) - x_{3d}(k+1) + \alpha_2(k) \tag{7.21}$$

$$z_4(k+1) = z_4(k) + f_2(z_3(k)) - f_4(z_3(k), z_4(k)) + u_y(k) + \phi_2(x(k))\eta_2 \tag{7.22}$$

where in order to overcome the causality we have denoted $z_1(k+1) = f_3(z_1(k), z_2(k))$ and $z_3(k+1) = f_4(z_3(k), z_4(k))$.

Also considering (7.17) and (7.18), we can express $\alpha_1(k+1) = f_1(f_3(z_1(k), z_2(k)))$ and $\alpha_2(k+1) = f_2(f_4(z_3(k), z_4(k)))$.

Finally, We introduce the finite-time control law for the transformed system (7.19)-(7.22)

$$u_p(k) = -f_1(z_1(k)) - \phi_1(x(k))\eta_1 + f_1(f_3(z_1(k), z_2(k))) - \min\left(\frac{|z_2(k)|}{c}, |z_2(k)|^\gamma\right) \tag{7.23}$$

$$u_y(k) = -f_2(z_1(k)) - \phi_2(x(k))\eta_2 + f_2(f_4(z_3(k), z_4(k))) - \min\left(\frac{|z_4(k)|}{c}, |z_4(k)|^\gamma\right). \tag{7.24}$$

Remark 7.2 *The controllers $u_p(k)$ and $u_y(k)$ in equations* (7.23) *and* (7.24) *have been developed by representing the error $z_1(k)$ as $f_1(\cdot)$ and $f_2(\cdot)$, thereby expressing them as functions of all system states through a recursive process.*

The following theorem is presented to succinctly summarize our main result.

Theorem 7.3 *For the discrete-time nonlinear two-DOF helicopter system described by equations* (7.19)-(7.22) *under Assumptions 1, the application of the proposed control laws* (7.23) *and* (7.24)*, in conjunction with virtual control laws* (7.17) *and* (7.18)*, guarantees that the system's output trajectory will track the desired reference signal within a finite time.*

Proof: Utilizing the closed-loop system formulated in (7.19)-(7.22), a finite-time stability analysis will be performed, progressing from the last component to the first component of the subsystem. Furthermore, an assessment of the settling time will be offered. In this instance, the entire system will be divided into two cascade subsystems.

7.3.1 Subsystem 1

Consider signals (7.19) and (7.20) from subsystem 1. Using control law (7.23), the last component (7.20) of the first subsystem is reduced to

$$z_2(k+1) = z_2(k) - \min\left(\frac{|z_2(k)|}{c}, |z_2(k)|^{\gamma}\right). \tag{7.25}$$

Consider the Lyapunov function as $V_1(z) = z_2^2(k)$. Given that $|z_2(0)| > c^{\frac{1}{1-\gamma}}$ (If $|z_2(0)| \leq c^{\frac{1}{1-\gamma}}$ and $z_2(0) \neq 0$, then $z_2(k) = 0$ will lead to (7.25) FTS with $K(z_{20}) = 1$). Then, we have:

$$\Delta V_1(z) = \left[z_2(k) - \min\left(\frac{|z_2(k)|}{c}, |z_2(k)|^{\gamma}\right)\right]^2 - z_2^2(k) \leq -c\min\left\{\frac{V_1(k)}{c}, V_1(k)^{\gamma}\right\}.$$

one can obtain the settling time function as [20]

$$K(z_{20}) \leq \left\lceil \log_{[1-cV(z_{20})^{\gamma-1}]} \frac{c^{\frac{1}{1-\gamma}}}{V(z_{20})} \right\rceil + 1,$$

such that $k > K(z_{20}), z_2(k) = 0$ and second component (7.19) of the first subsystem will reduce to

$$z_1(k+1) = z_1(k) - \min\left(\frac{|z_1(k)|}{c}, |z_1(k)|^{\gamma}\right). \tag{7.26}$$

Similar to the first component, consider $V_2(k) = z_1^2(k)$. By performing a similar analysis as above, it is evident that if $|z_1(K(z_{20}))| \leq c^{\frac{1}{1-\gamma}}$, $K(z_{10}) = K(z_{20}) + 1$ and if $|z_1(K(z_{20}))| > c^{\frac{1}{1-\gamma}}$

$$K(z_{10}) \leq \left\lceil \log_{[1-cV(z_{10})^{\gamma-1}]} \frac{c^{\frac{1}{1-\gamma}}}{V(z_{10})} \right\rceil + 1 + K(z_{20}),$$

will ensure that at $k > K(z_{10}), z_1(k) = 0$ and $z_2(k) = 0$. Using (7.13), we got $x_1(k) = x_{1d}(k)\ \forall\ k > K(z_{10})$, which shows finite-time tracking of reference signal $x_{1d}(k)$.

7.3.2 Subsystem 2

Consider signals (7.21) and (7.22) from subsystem 2. Using control law (7.24), the last component (7.22) of the second subsystem is reduced to

$$z_4(k+1) = z_4(k) - \min\left(\frac{|z_4(k)|}{c}, |z_4(k)|^{\gamma}\right). \tag{7.27}$$

Similar to subsystem 1, using $V_3(k) = z_4^2(k)$ shows that if $|z_4(0)| \leq c^{\frac{1}{1-\gamma}}$ and $z_4(0) \neq 0$, then using [20] $z_4(k) = 0$ will lead to (7.27) FTS with $K(z_{40}) = 1$ for $|z_4(0)| \leq c^{\frac{1}{1-\gamma}}$. Otherwise, if $|z_4(0)| > c^{\frac{1}{1-\gamma}}$ than

$$K(z_{40}) \leq \left\lceil \log_{[1-cV(z_{40})^{\gamma-1}]} \frac{c^{\frac{1}{1-\gamma}}}{V(z_{40})} \right\rceil + 1,$$

such that $z_4(k) = 0 \; \forall \; k > K(z_{40})$ and (7.21) will reduce to

$$z_3(k+1) = z_3(k) - \min\left(\frac{|z_3(k)|}{c}, |z_3(k)|^{\gamma}\right). \tag{7.28}$$

Also, consider $V_4(k) = z_3^2(k)$. Similar to subsystem 1 if $|z_3(K(z_{40}))| \leq c^{\frac{1}{1-\gamma}}$ will lead to $K(z_{30}) = K(z_{40}) + 1$ otherwise $K(z_{30}) \leq \left\lceil \log_{[1-cV(z_{30})^{\gamma-1}]} \frac{c^{\frac{1}{1-\gamma}}}{V(z_{30})} \right\rceil + K(z_{40}) + 1$ such that $\forall \; k > K(z_{30}), \; z_4(k) = 0$ and using (7.15) we have $\forall \; k > K(z_{30}), \; x_3(k) = x_{3d}(k)$ and $x_1(k) = x_{1d}(k)$ insures finite-time of tracking of reference signals. Hence, the overall system settling time will be $K(z_0)$= Max$[K(z_{30}), K(z_{10})]$. Therefore, $z(k)$=0 is finite-time stable, which completes the proof.

Remark 7.4 *This paper introduces a finite-time recursive backstepping control framework for a two-DOF helicopter system, differentiating itself from previous methods using NN-based approximation [69]. Our approach, utilizing variable substitution techniques, establishes a direct connection between the system states $x_i(k)$ and the controlled errors $z_i(k)$, overcoming challenges associated with causality.*

7.4 Result Discussion

A set of simulations and experiments was undertaken to evaluate the efficacy of the finite-time backstepping feedback control strategy devised in this study. The system parameters for the two-degree-of-freedom (2-DOF) helicopter system are derived from [68]. In this study, we initialized the two-DOF helicopter with $x_1(0) = -0.72$rad and $x_3(0) = 0.5$rad. The desired reference trajectory is defined as $x_{1d}(k) = 0.2\sin(2\pi 0.05k)$ and $x_{3d}(k) = 0.5\sin(2\pi 0.05k)$, adhering to Assumption 1. The control design parameters are set to $\gamma = 0.8$ and $c = 0.5$ with a sampling period of $h = 0.05$.

The simulation results with the proposed finite-time backstepping feedback control strategy are depicted in Fig. 7.2, showcasing the successful attainment of the desired pitch and yaw angle tracking within a finite time. In Fig. 7.2a and Fig. 7.2b, the tracking

of pitch angle $x_1(k)$ and yaw angle $x_3(k)$ is illustrated, respectively. The pitch tracking error $z_1(k)$ and yaw tracking error $z_3(k)$ are presented in Fig. 7.3a and Fig. 7.3b Fig. 7.4a and Fig. 7.4b depict the required control input. To reinforce this concept, we conducted a comparison with a control strategy developed in [10], as illustrated in Fig. 7.5 In Fig. 7.5a and Fig. 7.5b comparison of the proposed control scheme with [10] for the desired pitch and yaw angle tracking is presented. The results obtained from the comparison highlight the superiority of the proposed approach.

To validate both the practical feasibility and effectiveness of the proposed control strategy, we also conduct experimental validation using Quanser's two DOF helicopter test beds, building upon the insights gained from the simulation results. The experimental setup is depicted in Fig.7.1 Employing identical reference signals and control parameter values as used in the simulations, we execute the experiments, and the corresponding experimental results presented in Fig.7.6 illustrate the successful achievement of the desired pitch and yaw angle tracking. The corresponding pitch angle and yaw angle tracking errors are displayed in 7.6a and 7.6b, respectively.

7.5 Conclusion

In this concise presentation, we introduce a discrete-time recursive backstepping controller tailored for a 2-DOF helicopter, ensuring the tracking of pitch and yaw angle reference trajectories within a finite time frame. We consider the mathematical representation of the 2-DOF helicopter system, based on Euler-Lagrange equations, along with its Euler-based discretizations model. The introduced discrete-time recursive backstepping controller provides a systematic approach to achieve finite-time tracking. Simulations, along with experimental demonstrations on a Quanser 2-DOF helicopter, highlight the effectiveness and control potential of our proposed controller. As part of future work, the oscillatory behavior observed during the transient phase will be specifically addressed, with the aim of reducing transient oscillations to further enhance the overall performance.

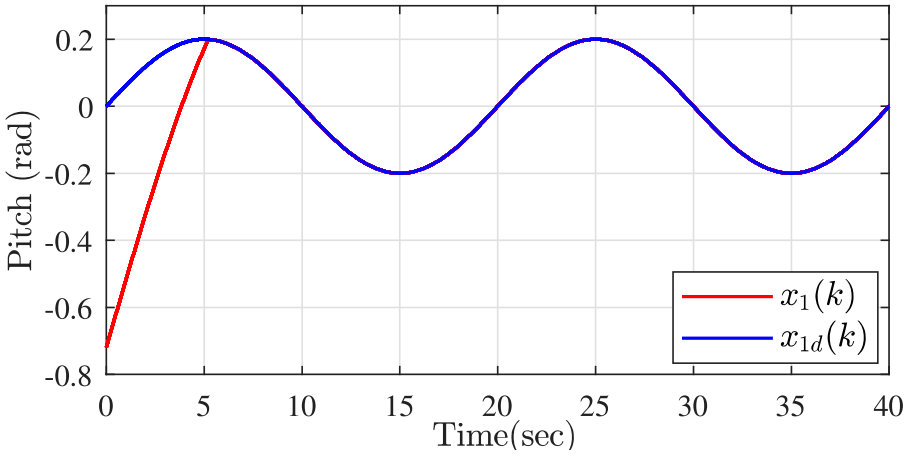

(a) Simulation results pitch angle.

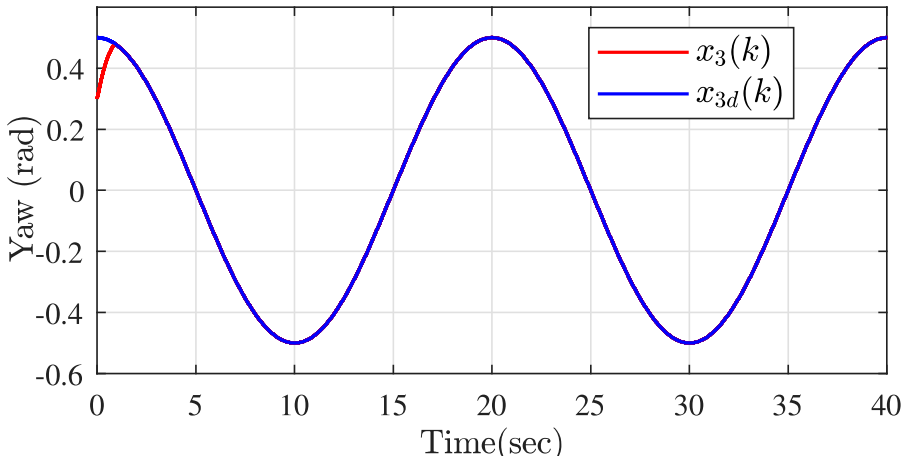

(b) Simulation results Yaw angle

Figure 7.2: Simulation result 2 DOF system

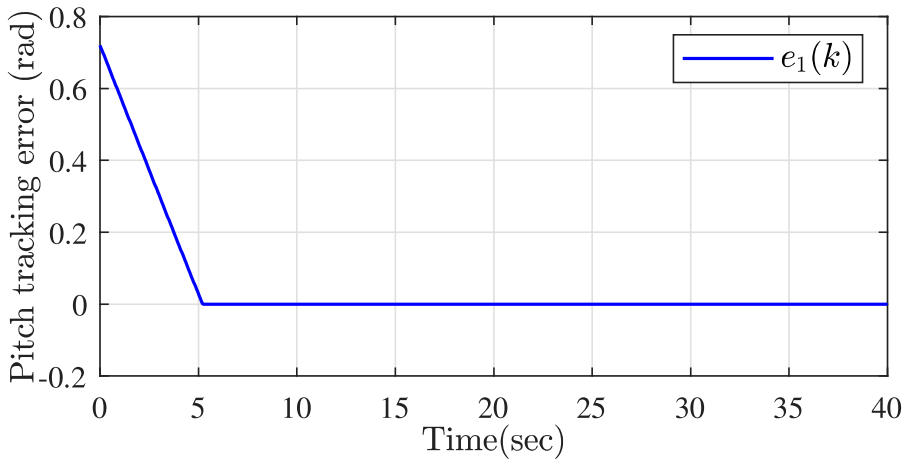

(a) Simulation result pitch error

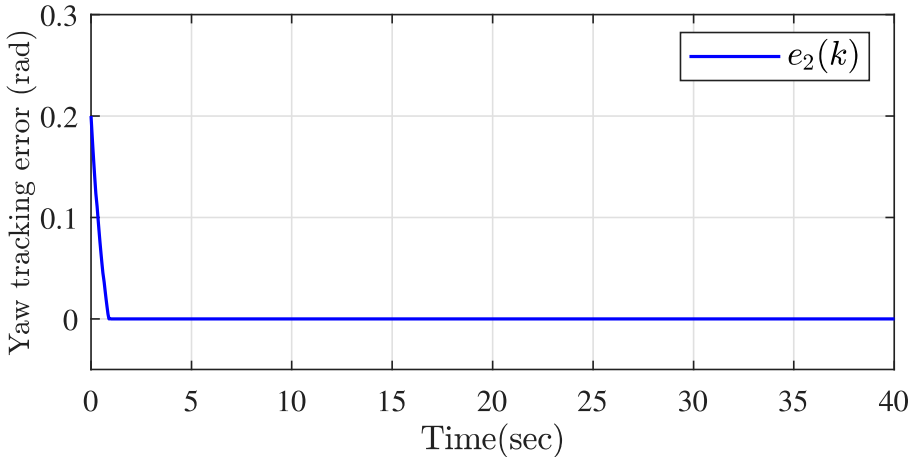

(b) Simulation result yaw error

Figure 7.3: Simulation result 2 DOF system

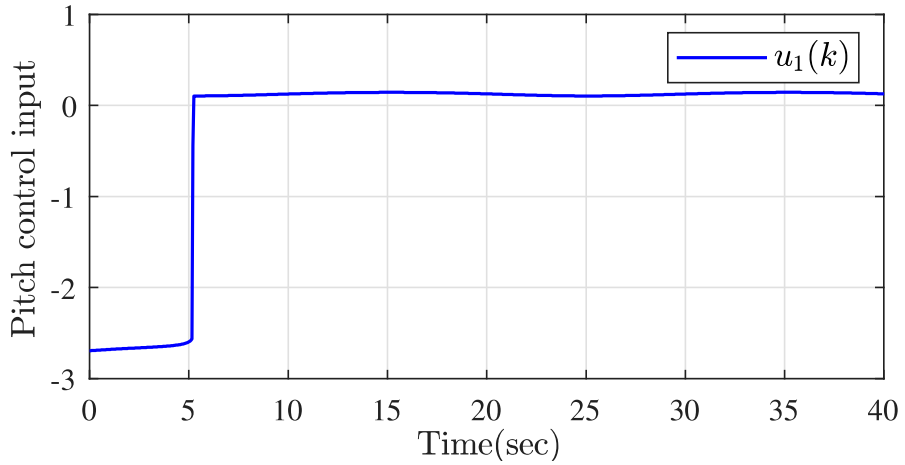

(a) Simulation result pitch control input

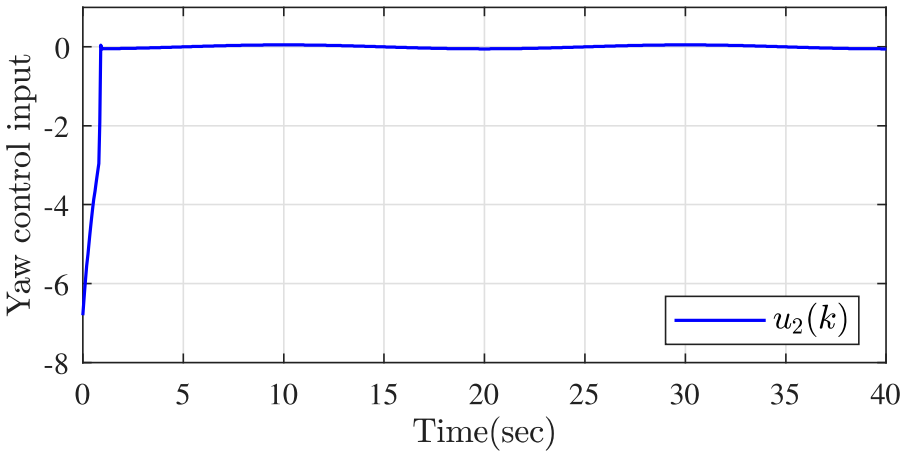

(b) Simulation result yaw control input

Figure 7.4: Simulation result 2 DOF system

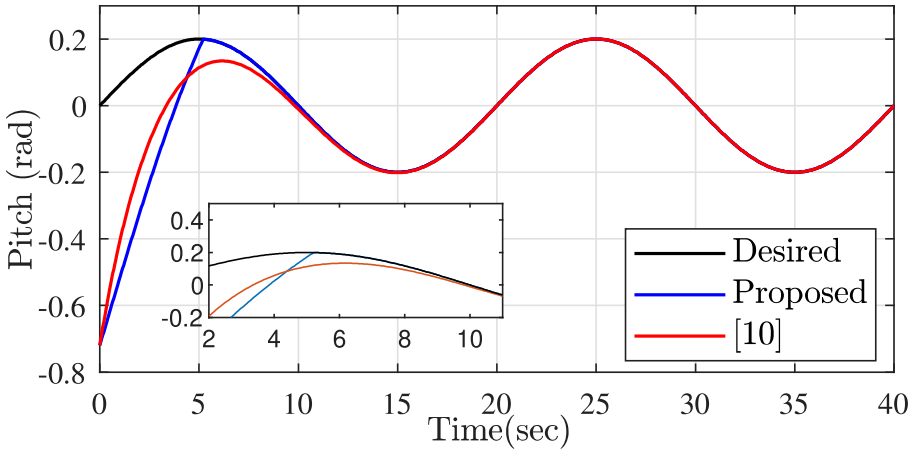

(a) Performance comparison for pitch angle between developed control and [10]

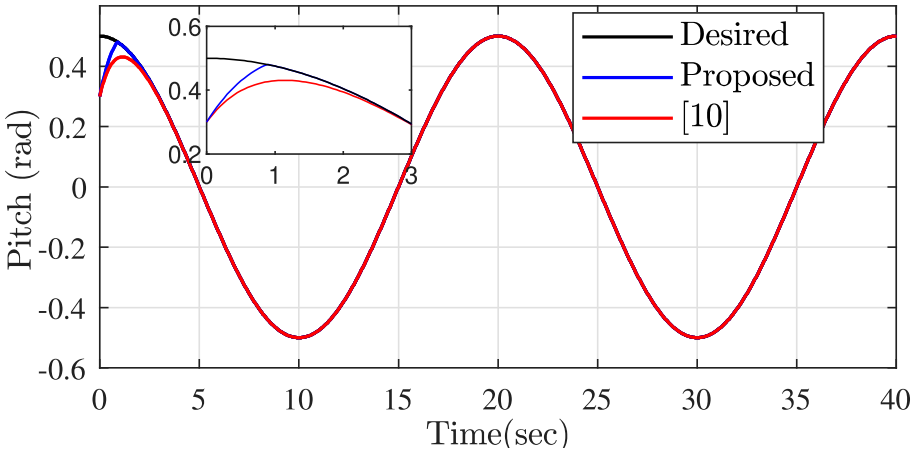

(b) Performance comparison for yaw angle between developed control and [10]

Figure 7.5: Simulation result comparison for 2 DOF system [10]

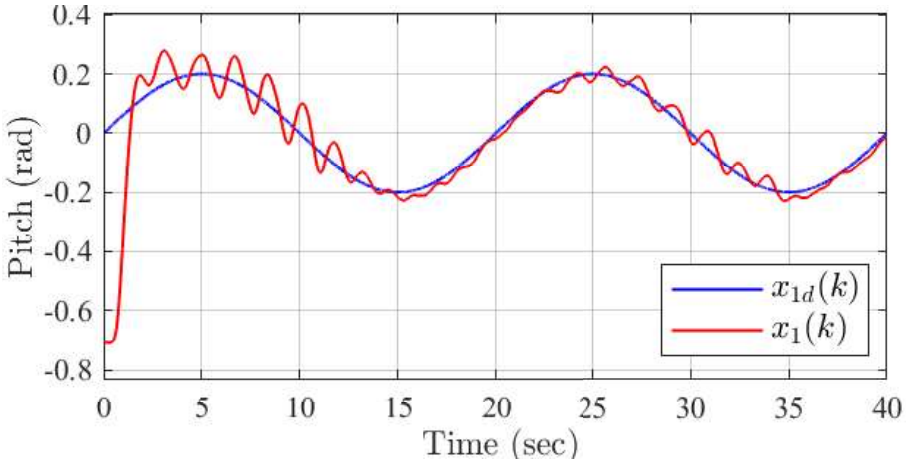

(a) Experimental result tracking pitch angle

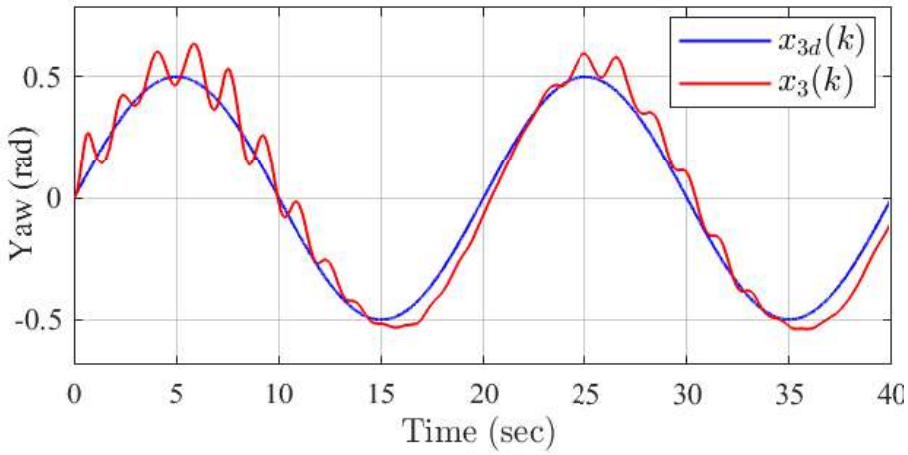

(b) Experimental result tracking yaw angle

Figure 7.6: Experimental result tracking 2 DOF system